UC San Diego

Adding new ingredients to the recipe of plasma soup: stochasticity, toroidicity, and nonlocality

Presenter: Mingyun Cao

Committee in charge:
Professor Patrick H. Diamond, Chair
Professor Daniel P. Arovas
Professor Michael L. Norman
Professor George R. Tynan

Dissertation defense | June 19, 2025

Contents

Introduction: new elements in plasma turbulence dynamics

Magnetic confinement fusion

- Nuclear fusion is a promising energy source.
  - ${}^2_1\mathrm{D} + {}^3_1\mathrm{T} \rightarrow {}^4_2\mathrm{He} + {}^1_0\mathrm{n}$
- Lawson criterion (for D-T fusion):
  - $nT\tau_E \geq 3 \times 10^{21}\ \mathrm{keV\ s/m^3}$.
  - Confine high T fuels of certain n for a certain period of time τ_E.
- Fusion reaction requires high T.
  - For D-T fusion, $T \sim 10\ \mathrm{keV}$.
  - Fuels become plasma (ions + electrons).

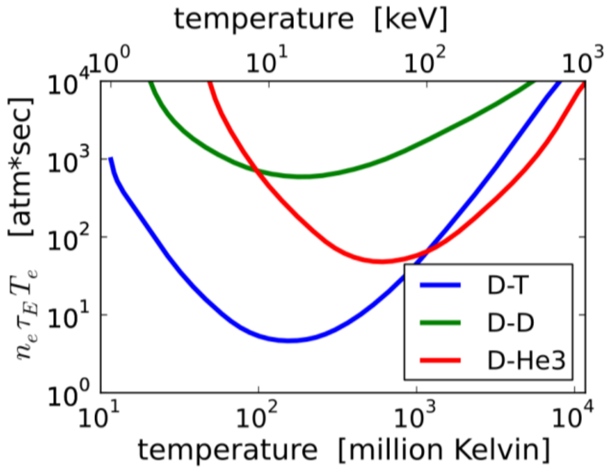

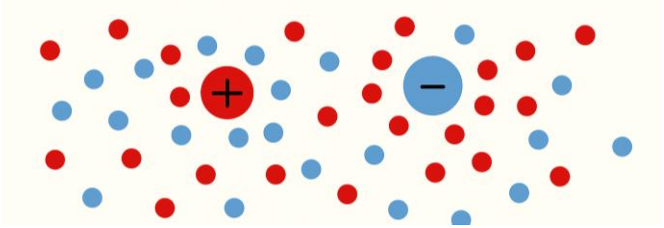

Magnetic confinement fusion

UC San Diego

- Idea: use magnetic field to build an intangible cage.
- Tokamak (**To**roidal **Cha**mber with **Ma**gnetic **C**oils).
- Feature: resemble a “doughnut”.
  - Strong toroidal magnetic field B_T.
  - Strong toroidal plasma current $\rightarrow B_\theta$.
  - Winding magnetic field lines.
  - Aspect ratio $R/a \sim 3-4$.
  - Safety factor $1 < q = \frac{rB_T}{RB_\theta} < \sim 3-4$.

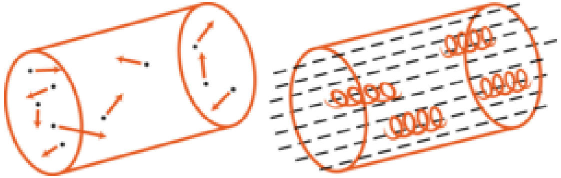

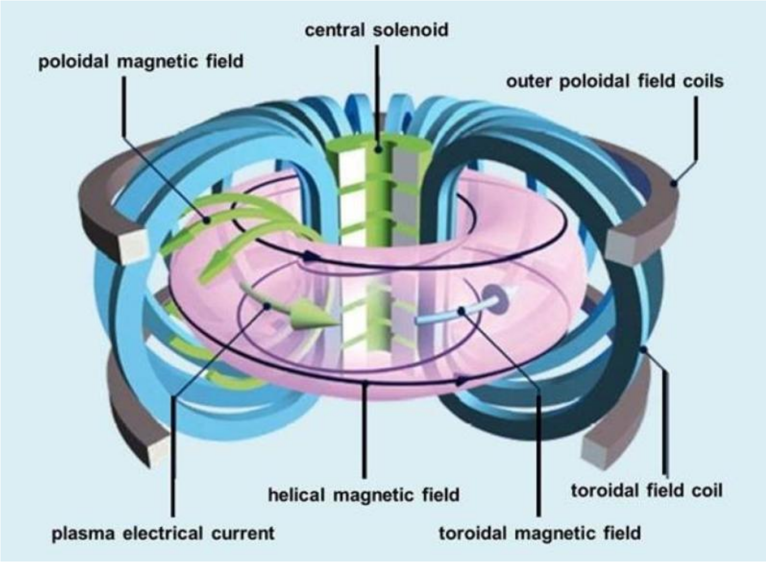

Turbulent transport in tokamaks

- τ_E: highest leverage parameter for capital cost.
- Core problem: plasma turbulence & turbulent transport.
- In 1982: τ_E doubles in high-confinement mode (H-mode).
- Plasma turbulence is regulated by zonal flow.

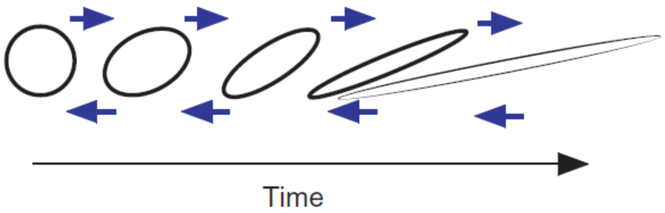

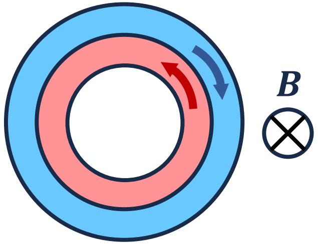

- $P > P_{LH} \Rightarrow$ formation of edge transport barrier.
- Predator (zonal flow)–prey (drift wave turbulence) model

Z. Lin, 1998, Science

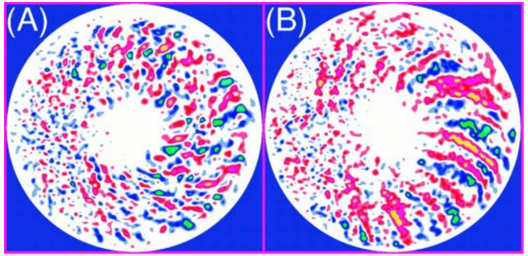

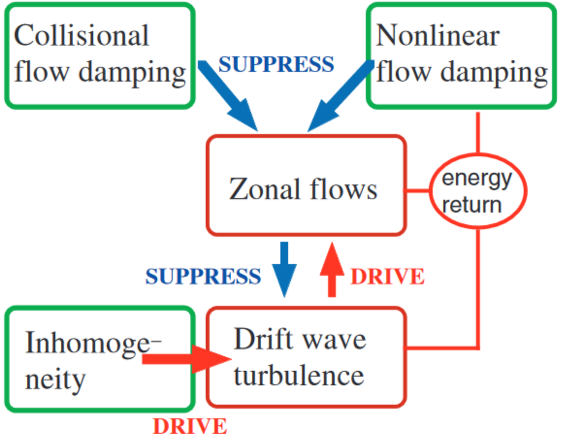

P.H. Diamond, 2005, PPCF

New elements of plasma turbulence

- Confinement is not the whole story.
- Tokamak is not an isolated system.
- Trade-off among confinement, heating power, and boundary protection.

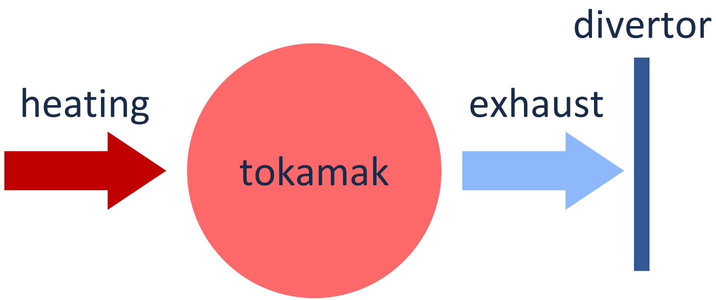

- Novel experimental phenomena demand deeper research on plasma turbulence.
- Features of existing theories:
  - Object: **an ensemble of waves**
  - Configuration: **a slab configuration**
  - Field: **a regular magnetic field**

V.S.

- Reality:
  - **Structures co-exist with waves**
  - **Tokamak is a torus**
  - **Fields could be chaotic**

Element 1: stochasticity

- Nonuniform winding rate $q(r)$: nested magnetic surfaces.
- KAM: with (intr./extr.) magnetic perturbations,
  - Resonant surfaces (q is rational) are destroyed.
  - Nonresonant surfaces (q is irrational) survive.
- Island chains develop on resonant surfaces.
- Field lines become stochastic when

$$\sigma_{\text{Chirikov}} = \frac{\delta_1+\delta_2}{\Delta_{12}} > 1$$

- Plasma dynamics must be reexamined to account for the presence of stochasticity.

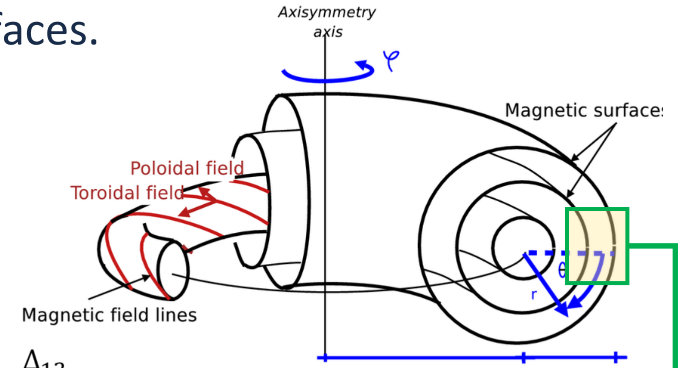

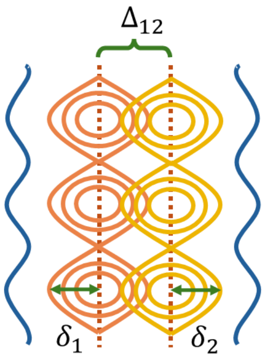

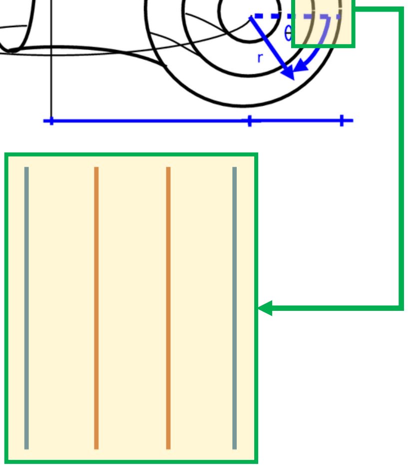

Element 2: toroidicity

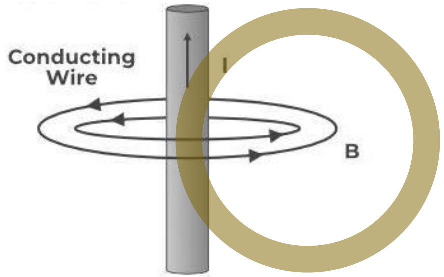

Ampère's law

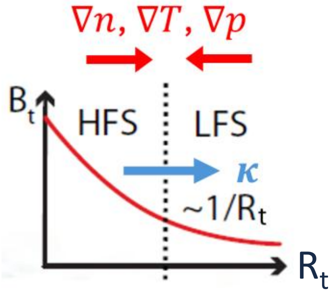

- Toroidal geometry of the tokamak ⇒
  - B_t on the inboard side is stronger.
  - B_t has a curvature directed outward.
- Poloidal symmetry is broken as
  - On high-field-side (HFS): $\boldsymbol{\kappa} \cdot \nabla p > 0$
  - On low-field-side (LFS): $\boldsymbol{\kappa} \cdot \nabla p < 0$
- Instabilities are easier to develop on LFS.

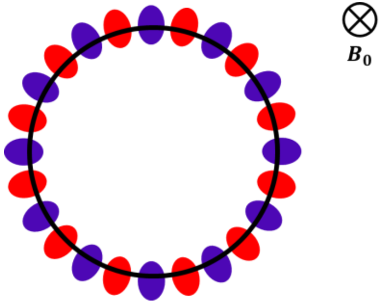

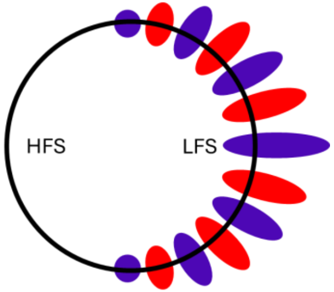

- Toroidicity results in broader mode structure (ballooning mode).
  - Toroidicity effect should be blended in along with stochasticity.

Element 3: nonlocality

- Diffusive description of transport in tokamaks is subjected to challenge.
  - Fickian formulation ($\Gamma_Q = -D\nabla Q$) fails.
- Convective transport may arise from coherent structures (blobs & voids) generated from edge gradient relaxation events (GREs).
- Blob/void: plasma filaments with +/- high $\tilde{n}$.

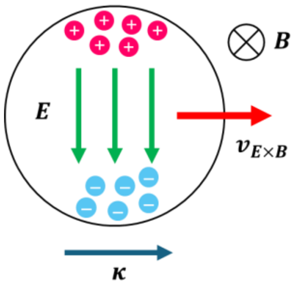

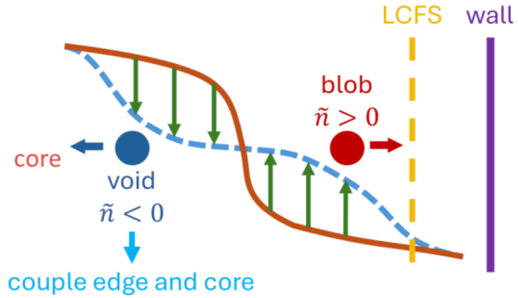

T. Long, 2024, NF

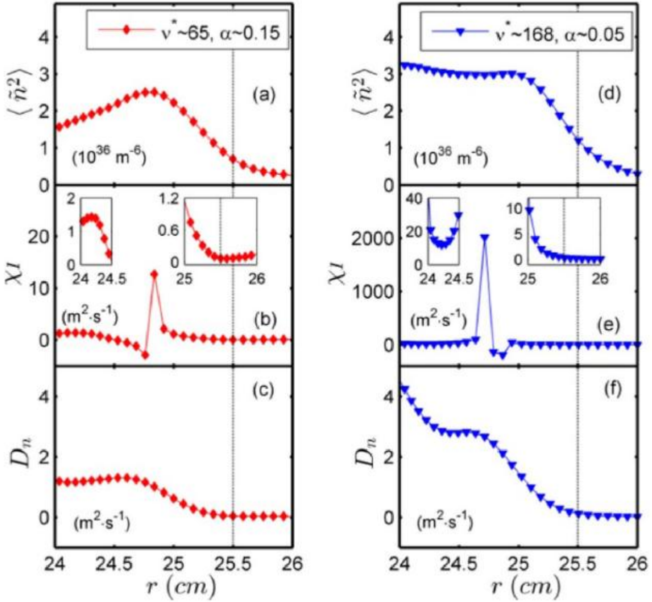

- A nonlocal theory is required.

Roadmap

- Target: extending the existing framework of plasma turbulence theory.
- Plasma turbulence: a soup including waves, structures, etc.
- In other words: adding new ingredients to the recipe of plasma soup!

How stochastic magnetic fields affect instability and turbulent relaxation

How toroidicity effects modify the story of plasma in stochastic fields

How inward-moving voids lead to the coupling of core and edge plasmas

Ingredient 1: stochasticity

Instability and turbulent relaxation in a stochastic magnetic field

Motivation

- Resonant magnetic perturbations (RMPs) is adopted to mitigate and suppress edge-localized modes (ELMs) by exciting a stochastic magnetic field at the plasma edge.
- RMPs raise the L-H transition power threshold P_{LH}.

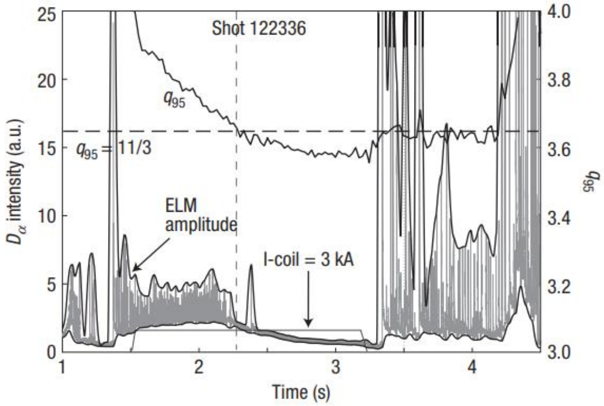

Suppression of ELMs by RMPs
T.E. Evans, 2015, Nature Physics

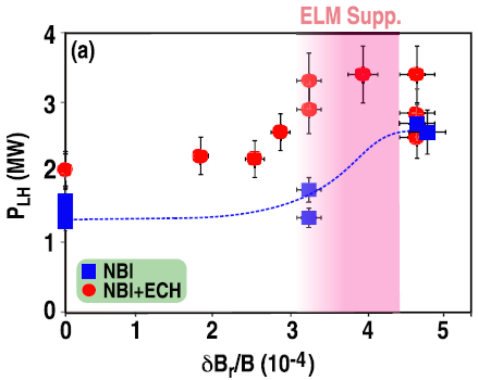

RMPs raise P_{LH}
L. Schmitz, 2019, NF

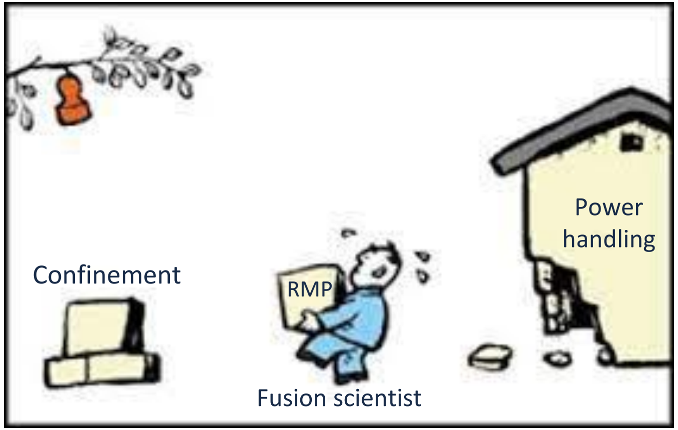

Scope

- New trend: a trade-off among confinement, boundary control and power handling.
- Turbulence dynamics must be reformulated to include extrinsic stochasticity.
- Question: how does stochastic magnetic field modify the instability process?
- Requirement: capture the key physics while remaining analytically tractable.

  a) Examine a simple MHD instability, resistive interchange mode (low-$\boldsymbol{k}$).

  b) Incorporate a static, ambient stochastic magnetic field (high-$\boldsymbol{k}$).

  c) Maintain the quasi-neutrality ($\nabla \cdot \boldsymbol{J} = 0$) at all scales $\Rightarrow$ ensure generality.
- The dynamics is intrinsically multi-scale $\Rightarrow$ feedback loop.

Model development

- Formulation of the resistive interchange mode:
  - Vorticity equation: $-(\rho_0/B_0^2)\partial_t\nabla_\perp^2\varphi - (\kappa/B_0)\partial_y p + \boldsymbol{b_0}\cdot\nabla J_\parallel = 0 \Leftrightarrow \nabla\cdot\boldsymbol{J} = 0.$
  - Ohm's law: $E_\parallel = -\boldsymbol{b_0}\cdot\nabla\varphi = \eta J_\parallel.$
  - Pressure equation: $\partial_t p - \nabla\varphi\times\boldsymbol{b_0}/B_0\cdot\nabla p_0 = 0.$

ρ_0: mean plasma density;
B_0: mean magnetic field;
κ: magnetic curvature;
φ: electrostatic potential.

- Magnetic perturbations: $\widetilde{\boldsymbol{b}} = \widetilde{\boldsymbol{B}}_\perp/B_0 = \sum_{m_1n_1}\widetilde{\boldsymbol{b}}_{\boldsymbol{k_1}}(x')e^{i(m_1\theta-n_1\phi)}\ (x' = r - r_{m_1n_1}).$

parallel gradient

$$\nabla_\parallel = \boldsymbol{b_0}\cdot\nabla$$

$$\downarrow$$

$$\nabla_\parallel = \nabla_\parallel^{(0)} + \widetilde{\boldsymbol{b}}\cdot\nabla$$

$\vec{k}\cdot\vec{B}_0 = 0$

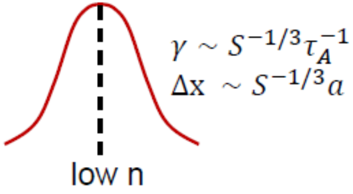

single test mode

+

Spectrum of prescribed static magnetic fluctuations

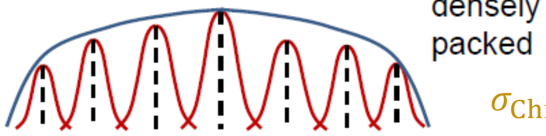

$\sigma_{\text{Chirikov}} \gg 1$

$|b_{k'}|^2 = |b_0|^2 S(k_\theta)\Gamma\big((r - r_{k'})/w_{k'}\big)$

Model development

- Constraint: maintaining $\nabla \cdot \boldsymbol{J} = 0$ at all scales.
- $\tilde{\boldsymbol{b}}$ leads to parallel current density fluctuations.

$$\nabla_{\parallel} \widetilde{J}_{\parallel} = -\frac{1}{\eta}\left\{\nabla_{\parallel}^{(0)}\left[(\tilde{\boldsymbol{b}} \cdot \nabla_{\perp})\varphi\right] + (\tilde{\boldsymbol{b}} \cdot \nabla_{\perp})\nabla_{\parallel}^{(0)}\varphi\right\} \neq 0$$

- $\tilde{J}_{\perp}$ is driven to balance $\tilde{J}_{\parallel} \Rightarrow \nabla \cdot (\tilde{J}_{\perp} + \tilde{J}_{\parallel}) = 0$.
- Indication:
  - $\tilde{\varphi}$: (high-$\boldsymbol{k}$) microturbulence.
  - Or small-scale convective cells.
  - Increased "spatial roughness"?

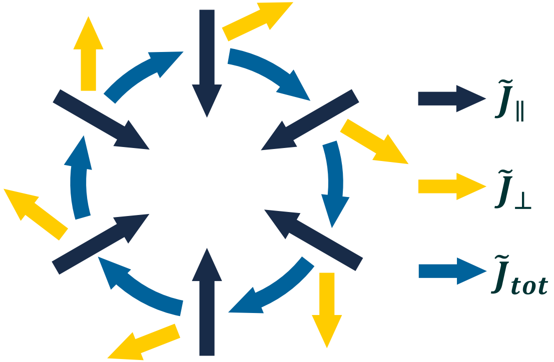

P. Beyer, 1998, PoP

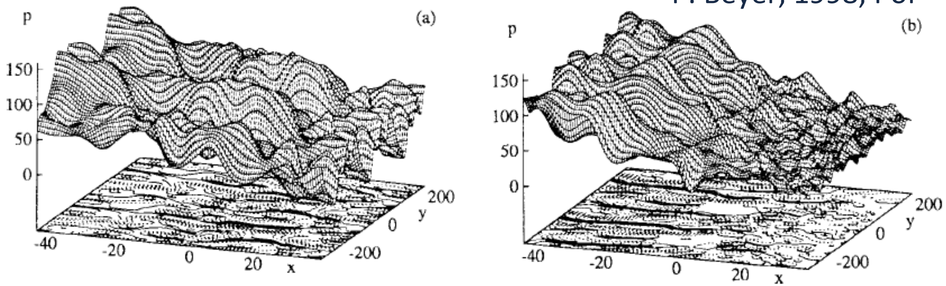

Plasma pressure without (a) and with (b) RMPs

Model development

- The resulting dynamics are intrinsically multi-scale.

$$\left(\frac{\partial}{\partial t}+\tilde{\boldsymbol{v}}\cdot\nabla\right)\nabla_\perp^2(\bar{\varphi}+\tilde{\varphi})=\frac{\eta S}{\tau_A}\nabla_\parallel J_\parallel-\frac{\kappa B_0}{\rho_0}\frac{\partial(\bar{p}_1+\tilde{p}_1)}{\partial y},$$

$$\left(\frac{\partial}{\partial t}+\tilde{\boldsymbol{v}}\cdot\nabla\right)(\bar{p}_1+\tilde{p}_1)-\frac{\nabla(\bar{\varphi}+\tilde{\varphi})\times\hat{\boldsymbol{z}}}{B_0}\cdot\nabla p_0=0,$$

$$\eta J_\parallel=-\nabla_\parallel(\bar{\varphi}+\tilde{\varphi}).$$

$\bar{\varphi}$: low-$\boldsymbol{k}$ test mode;

$\tilde{\varphi}$: high-$\boldsymbol{k}$ microturbulence;

$S=\tau_R/\tau_A$;

$\tau_A=a(4\pi\rho_0)^{1/2}/B_0$;

$\tau_R=4\pi a^2/\eta$.

- Technique: method of averaging

$$\bar{A}=\langle A\rangle=\left(\frac{1}{2\pi}\right)^2\iint d\theta d\phi e^{-i(m\theta-n\phi)}A$$

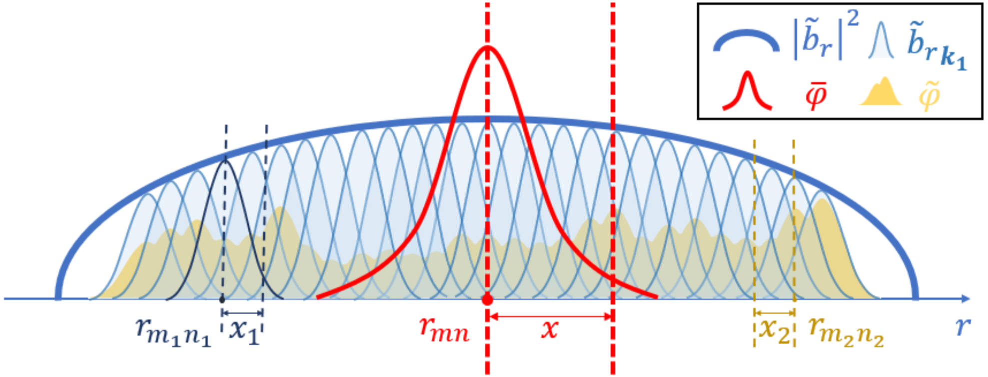

Model development

- Full set of equations:

$$① \left[\frac{\partial}{\partial t} + \tilde{\boldsymbol{v}}\cdot\nabla\right]\nabla_\perp^2 \bar{\varphi} = -\frac{S}{\tau_A}\left[\nabla_\parallel^{(0)^2}\bar{\varphi} + \underbrace{\left(\nabla_\perp\cdot\langle\tilde{\boldsymbol{b}}\tilde{\boldsymbol{b}}\rangle\right)\cdot\nabla_\perp\bar{\varphi}}_{(a)} + \underbrace{\left\langle\nabla_\parallel^{(0)}\tilde{\boldsymbol{b}}\cdot\nabla_\perp\tilde{\varphi}\right\rangle}_{(b)} + \underbrace{\left\langle\left(\tilde{\boldsymbol{b}}\cdot\nabla_\perp\right)\nabla_{\parallel'}^{(0)}\tilde{\varphi}\right\rangle}_{(c)}\right] - \frac{gB_0}{\rho_0}\frac{\partial\bar{p}_1}{\partial y},$$

$$② \left[\frac{\partial}{\partial t} + \tilde{\boldsymbol{v}}\cdot\nabla\right]\nabla_\perp^2 \tilde{\varphi} = -\frac{S}{\tau_A}\left[\nabla_\parallel^{(0)^2}\tilde{\varphi} + \underbrace{\left(\tilde{\boldsymbol{b}}\cdot\nabla_\perp\right)\nabla_\parallel^{(0)}\bar{\varphi}}_{(\alpha)} + \underbrace{\nabla_\parallel^{(0)}\left(\tilde{\boldsymbol{b}}\cdot\nabla_\perp\right)\bar{\varphi}}_{(\beta)}\right] - \frac{gB_0}{\rho_0}\frac{\partial\tilde{p}_1}{\partial y},$$

$\longrightarrow$ Relate $\tilde{\varphi}$ to $\tilde{\boldsymbol{b}}$

$$③ \left[\frac{\partial}{\partial t} + \tilde{\boldsymbol{v}}\cdot\nabla\right]\bar{p}_1 - \frac{\nabla\bar{\varphi}\times\hat{\mathbf{z}}}{B_0}\cdot\nabla p_0 = 0,$$

$$④ \left[\frac{\partial}{\partial t} + \tilde{\boldsymbol{v}}\cdot\nabla\right]\tilde{p}_1 - \frac{\nabla\tilde{\varphi}\times\mathbf{z}}{B_0}\cdot\nabla p_0 = 0,$$

replaced by $\boxed{-\nu_T\nabla_\perp^2 \text{ or } \chi_T\nabla_\perp^2}$

leads to

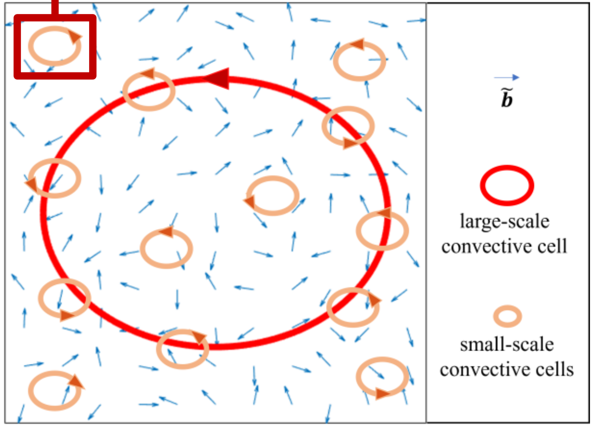

- Adopted assumptions: $k \gg k_1$

drives

reacts

- $\bar{\varphi}$: slow interchange ($k_r \gg k_\theta$)
- $\tilde{\varphi}$: fast interchange ($k_{1\theta} \gg k_{1r}$)

Results

- Quasi-linear approach: $\tilde{\varphi}$ driven by beat of $\tilde{\boldsymbol{b}}$ and $\bar{\varphi}$.

→ Microturbulence locks on to the perturbed fields:

$$\langle \tilde{b}_r \tilde{v}_r \rangle = \pi^{\frac{1}{2}} \frac{k_\theta R r_{mn}}{L_S^2 B_0} \frac{S}{\tau_A} \bar{\varphi}_k(0) \times \int dk_{2\theta} |k_{2\theta}| k_{2\theta} \frac{c^2 Z^2 (k_\theta - k_{2\theta}) w_{k_2} o_{k_2}^2}{\Lambda_{k_2}^0 - \Lambda_{k_2}}$$

- When RMP is switched on, for edge turbulence, its
  - Bicoherence increases ⇒ $\tilde{\varphi}$ enhances nonlinear transfer.
  - Complexity decreases ⇒ turbulence becomes “noisier”.
- Jensen-Shannon complexity: white noise (low), chaos (high).

Increased bicoherence and decreased complexity in RMP ELM suppression phase

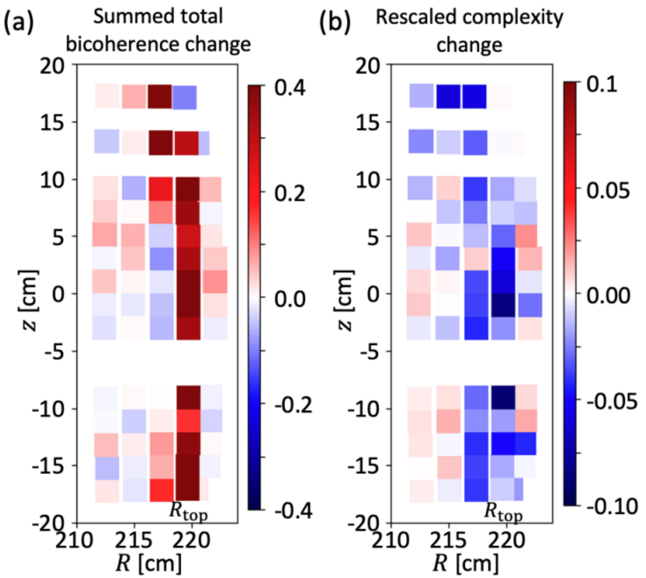

M.J. Choi, 2022, PoP

Results:

- The 1st order correction to the growth rate of the test mode:

$$\gamma_k^{(1)} \& = \underbrace{-\frac{1}{3}\frac{S}{\tau_{\mathrm{A}}}\left|\tilde{b}_r\right|^2}_{\substack{\text{magnetic}\\ \text{braking effect}}} \underbrace{-\frac{5}{6}\frac{\nu_T}{L_s^2}\left(\frac{\tau_{\mathrm{p}}\tau_\kappa}{\tau_{\mathrm{A}}^2}\right)^{1/3} S^{2/3}\tilde{k}_\theta^{2/3}}_{\text{turbulent damping}} \underbrace{-\frac{2\sqrt{2}}{3}\frac{\hat{I}S^{4/3}\tilde{k}_\theta^{4/3}}{\left(\tau_{\mathrm{p}}\tau_\kappa\tau_{\mathrm{A}}^4\right)^{1/3}}}_{\substack{\text{electrostatic}\\ \text{scattering}}} < 0$$

- Stochastic bending enhances plasma inertia ⇒ magnetic braking effect[1]

$$-\frac{S}{\tau_{\mathrm{A}}}\frac{k_\theta^2}{L_{\mathrm{s}}^2}\frac{d^2}{dk_x^2}\bar{\varphi}_{\boldsymbol{k}} + \left[\frac{S}{\tau_{\mathrm{A}}}\left|\tilde{b}_r\right|^2 + \underbrace{\boxed{\gamma_{\boldsymbol{k}}}}_{\text{inertia}}\right]k_x^2\bar{\varphi}_{\boldsymbol{k}} - \frac{\kappa p_0}{L_{\mathrm{p}}\rho_0}\frac{k_\theta^2}{\gamma_{\boldsymbol{k}}}\bar{\varphi}_{\boldsymbol{k}} = 0$$

- Net effect of a stochastic magnetic field on a large-scale mode is to reduce its growth.

1. P.H. Rutherford, 1973, PoF (Nonlinear tearing mode)

Results

- Growth of the small-scale convective cells is damped by turbulent viscosity ν_T.
  - Recall $\partial_t + \tilde{\boldsymbol{v}} \cdot \nabla \to \partial_t - \nu_T \nabla_\perp^2$. $\tilde{\varphi}$ is over-saturated if $\nu_T k_{1\theta}^2 > \gamma_{\boldsymbol{k}_1}^{(0)} = \left(c_s^2 \kappa / L_p\right)^{1/2}$
- Scaling of ν_T is calculated using a simple nonlinear closure theory:

$$\nu_T = \sum_{\boldsymbol{k}_2} \left|\tilde{v}_{\boldsymbol{k}_2}\right|^2 \tau_{\boldsymbol{k}_2}$$

c and $Z(k_{2\theta})$are normalization factor and spectrum of $\tilde{b}_{r_{\boldsymbol{k}_2}}$

- In the limit of $\nu_T k_{1\theta}^2 \gg \left(c_s^2 \kappa / L_p\right)^{1/2}$:

$$\nu_T = \left[\pi^{\frac{1}{2}} \frac{R r_{mn}}{B_0^2} \frac{k_\theta^2}{L_s^3} \left(\frac{S}{\tau_\mathrm{A}}\right)^2 \bar{\varphi}_{\boldsymbol{k}}^2(0) \int dk_{2\theta} \frac{c^2 Z^2 w_{\boldsymbol{k}_2} o_{\boldsymbol{k}_2}^2}{|k_{2\theta}|^5 \gamma_{\boldsymbol{k}_2}^{(0)}}\right]^{1/3}$$

Section summary

- $\nabla \cdot \boldsymbol{J} = 0$ at all scales ⇒ microturbulence.
- Large and small scales are interacted.
  - $\tilde{\varphi}$ driven by the beat of $\tilde{\boldsymbol{b}}$ and $\bar{\varphi}$.
  - $\bar{\varphi}$ damped and scattered by $\tilde{\varphi}$.
- $\tilde{\boldsymbol{b}}$ leads to a magnetic braking effect.
  - Enhances plasma inertia ⇒ a drag
- Net effect of $\tilde{\boldsymbol{b}}$ on interchange: stabilization.
- $\langle \tilde{b}_r \tilde{v}_r \rangle \neq 0$ ⇒ turbulence becomes noisier with RMPs ⇒ reduced J-S complexity.

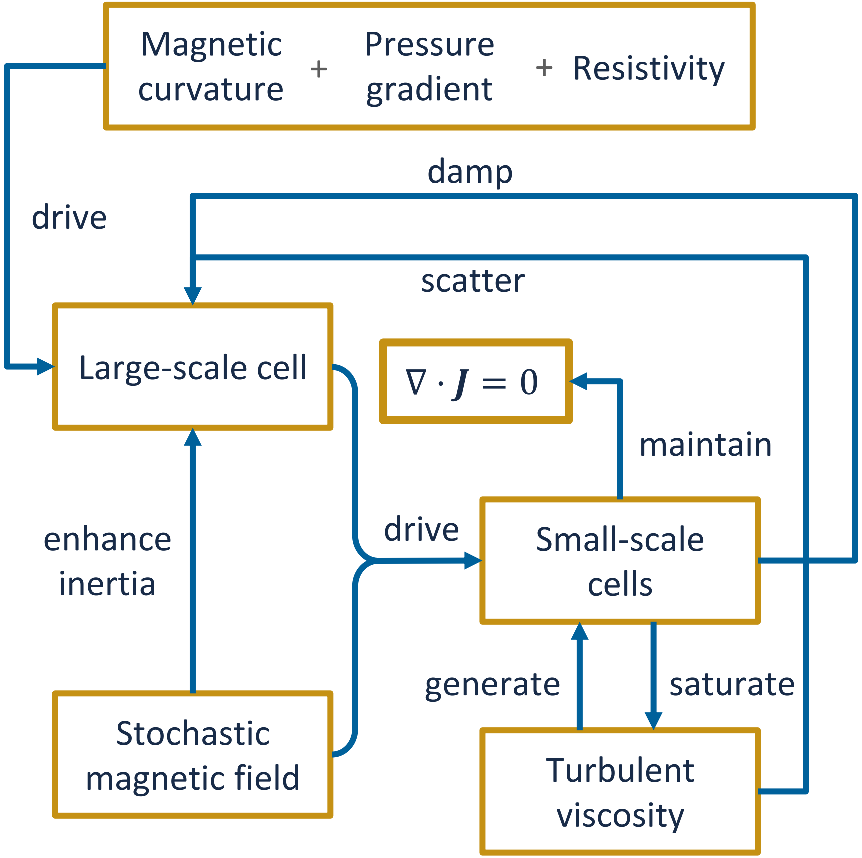

Ingredient 2: toroidicity

Quasi-mode evolution in a stochastic magnetic field

Motivation: from slab to torus

- RMPs: ELMs $\downarrow$, $P_{LH} \uparrow \Rightarrow$ study of resistive interchange in a stochastic magnetic field.
- Peeling-ballooning mode: a probable candidate for ELMs $\Rightarrow$ a more relevant instability.
- Target: a tractable theoretical model of ballooning mode in a stochastic field.
- Challenge: different geometries in ballooning mode and RMPs theories.

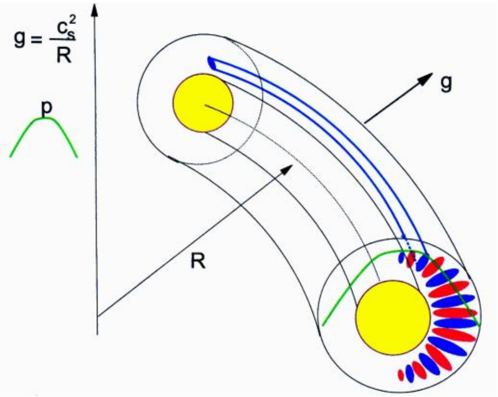

Ballooning mode

$\Updownarrow$

Toroidicity effect

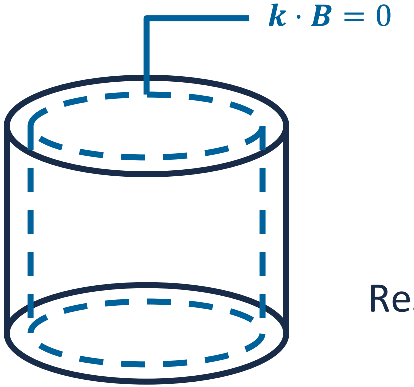

RMP

$\Updownarrow$

Resonant surfaces
in a **cylinder**

Counterpart of ballooning mode

- Two-step scheme: 1, find the counterpart of ballooning mode in the cylindrical geometry and study it; 2, generalize results to ballooning mode.
- Quasi-mode in a cylinder resembles ballooning mode in a torus: broad mode structure.
    - Ballooning mode: a coupling of localized poloidal harmonics.
    - Quasi-mode: a wave-packet of radially localized resistive interchange modes.

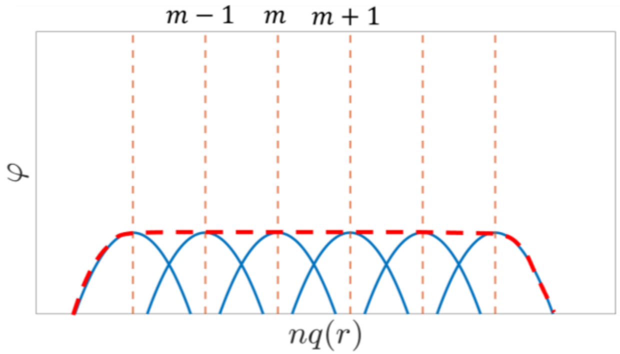

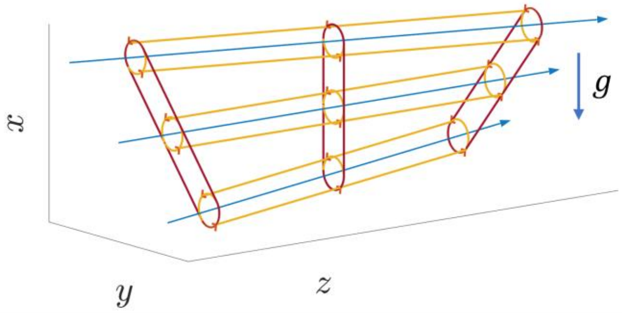

Physical picture: microturbulence

- Quasi-mode: a linear superposition of resistive interchange mode.
- Expect a similar physical picture: emergence of microturbulence.

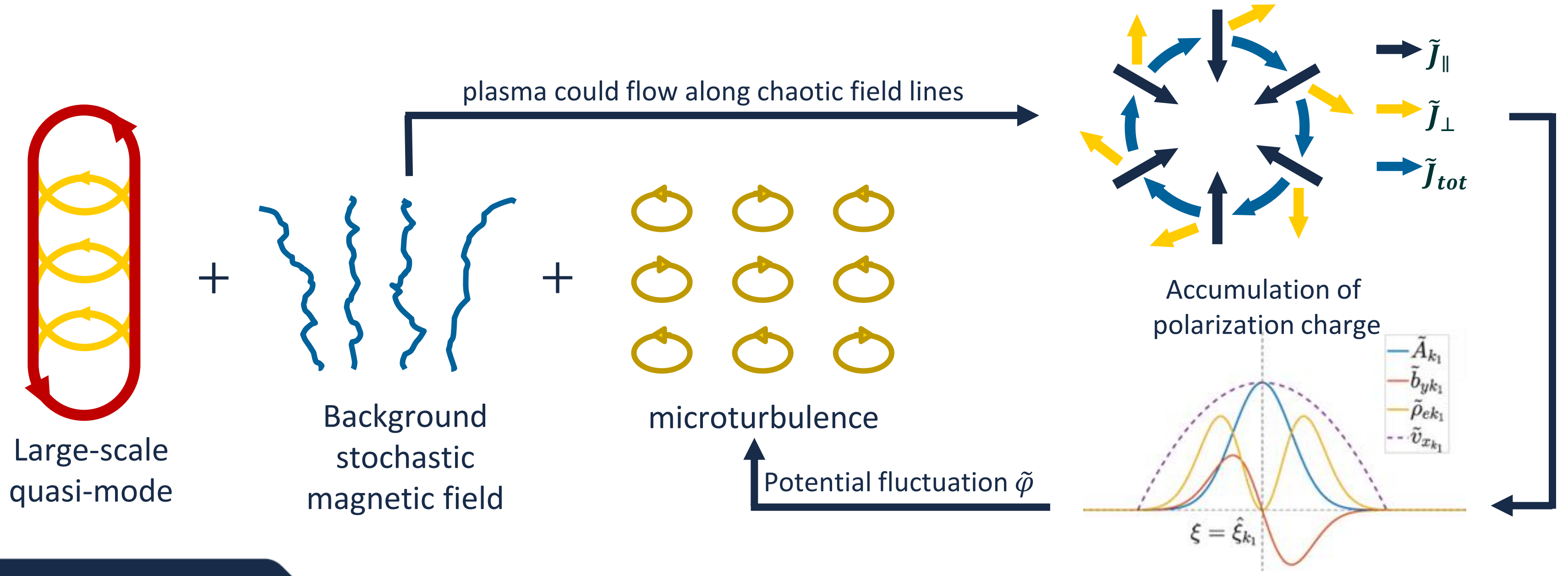

Key change: broad mode structure

- Formulation of quasi-mode dynamics:
  - Vorticity eqn : $\rho_0\left(\frac{\partial}{\partial t} - \boxed{\nu_T}\nabla_\perp^2\right)\nabla_\perp^2(\bar{\varphi} + \tilde{\varphi}) + \frac{B_0^2}{\eta}\left(\nabla_\parallel + \tilde{\boldsymbol{b}}\cdot\nabla_\perp\right)^2(\bar{\varphi} + \tilde{\varphi}) - gB_0\frac{\partial(\bar{\rho}+\tilde{\rho})}{\partial y} = 0$
  - Continuity eqn: $\left(\frac{\partial}{\partial t} - \boxed{D_T}\nabla_\perp^2\right)(\bar{\rho} + \tilde{\rho}) = -(\bar{v}_x + \tilde{v}_x)\alpha\rho_0$

$\tilde{\varphi}, \tilde{\rho}, \tilde{v}_x$: microturbulence
ν_T: turbulent viscosity

- Major difference: quasi-mode has a **much broader** radial mode structure.

→ A change in the spatial ordering of the system:

$$\boxed{\frac{1}{\bar{v}_x}\underbrace{\frac{\partial}{\partial \xi}\bar{\varphi}}_{=0}} \ll \frac{1}{\bar{v}_x}\frac{\partial}{\partial \zeta}\bar{\varphi} \ll \boxed{\frac{1}{\bar{v}_x}\frac{\partial}{\partial \chi}\bar{\varphi}} \ll \frac{1}{\tilde{v}_x}\frac{\partial}{\partial x}\tilde{\varphi} \ll \frac{1}{\tilde{v}_x}\frac{\partial}{\partial \chi}\tilde{\varphi}$$

switched

$$\frac{1}{\bar{v}_x}\frac{\partial}{\partial \zeta}\bar{\varphi} \ll \frac{1}{\tilde{v}_x}\frac{\partial}{\partial \zeta}\tilde{\varphi} \ll \frac{1}{\tilde{v}_x}\frac{\partial}{\partial \chi}\tilde{\varphi}$$

$$\nu_T k_y^2 \ll \gamma_{\boldsymbol{k}} \ll \gamma_{\boldsymbol{k}_1} < \nu_T k_{1y}^2$$

Results

- Along with $\langle \tilde{v}_x \tilde{b}_x \rangle$, a new correlation $\langle \tilde{v}_x \tilde{b}_y \rangle$ appears.

$$\langle \tilde{v}_x \tilde{b}_x \rangle = \frac{iL_yL_z}{(2\pi)^2} \int d\,k_{1y} \frac{s^2 k_y S \left| \tilde{A}_{0\boldsymbol{k}_1} \right|^2}{\tau_A \nu_T |k_{1y}|} \frac{12\sqrt{\pi} o_{\boldsymbol{k}_1}^2}{w'} \zeta \partial_\zeta \bar{v}_x$$

$$\langle \tilde{v}_x \tilde{b}_y \rangle = -\frac{iL_yL_z}{(2\pi)^2} \int dk_{1y} \frac{s^3 k_y S \left| \tilde{A}_{0\boldsymbol{k}_1} \right|^2}{\tau_A \nu_T |k_{1y}|} \frac{12\sqrt{\pi} o_{\boldsymbol{k}_1}^4}{w'} \zeta \bar{v}_x$$

$$\boxed{\frac{1}{\bar{v}_x} \underbrace{\frac{\partial}{\partial \xi} \bar{\varphi}}_{=0}} \ll \frac{1}{\bar{v}_x} \frac{\partial}{\partial \zeta} \bar{\varphi} \ll \boxed{\frac{1}{\bar{v}_x} \frac{\partial}{\partial \chi} \bar{\varphi}}$$

switched

- Scaling of turbulent viscosity ν_T becomes larger.

$$\nu_T = \sum_{\boldsymbol{k}_1} \left| \tilde{\boldsymbol{v}}_{\boldsymbol{k}_1} \right|^2 \tau_{\boldsymbol{k}_1} \cong \left[\frac{L_zL_y}{(2\pi)^2} \int dk_{1y} \frac{s^3 S^2 \left| \tilde{A}_{\boldsymbol{k}_1} \right|^2}{\tau_A^2 |k_{1y}|^3} \frac{4\sqrt{\pi} o_{\boldsymbol{k}_1}^2 \bar{v}_{x\boldsymbol{k}}(0)^2}{w'(\alpha g)^{1/2}} \left\{ \underbrace{2}_{\text{old}} + \underbrace{\left(\frac{k_{1y} o_{\boldsymbol{k}_2}^2}{k_y w_{\boldsymbol{k}} w'} \right)^2}_{\text{new}} \right\} \right]^{1/3}$$

Results

- The correction to the growth of the quasi-mode is

$$\gamma_{\boldsymbol{k}}^{(1)} = -\frac{5}{6}s^2\Delta^2\nu_T k_y^2\left(\underbrace{1+\frac{8}{5}\frac{1}{s^2\Delta^2}}_{\text{new}}\right) - \frac{1}{3}\frac{S}{\tau_A}\left((1-f)\left|\tilde{b}_x^2\right| \underbrace{+\frac{2}{s^2\Delta^2}\left|\tilde{b}_y^2\right|}_{\text{new}}\right)$$

- New terms arise because of the change in spatial ordering.
  - Turbulent viscosity damping: enhanced by larger ν_T.
  - Magnetic braking effect: weakened by microturbulence scattering.
  - New stabilization mechanism: reduction in the effective drive.
- Conclusion remains the same: effect of $\widetilde{\boldsymbol{b}}$ is to slow down the mode growth.

Section summary

- Lessons learned for ballooning mode dynamics (in presence of magnetic perturbations):
  - Stochastic magnetic field impedes the growth of ballooning mode.
    1. Enhancing the effective plasma inertia (magnetic braking effect)
    2. Reducing the effective drive
    3. Promoting turbulence damping
  - Microturbulence is driven and yields a turbulent background.
    1. $\nu_T^{\text{ballooning}} > \nu_T^{\text{interchange}}$
    2. Electrostatic scattering is destabilizing ⇒ opposite to result for interchange.

Ingredient 3: nonlocality

Physics of edge-core coupling by inward turbulence propagation

Background: voids in tokamaks

- Turbulence: a multi-ingredient concoction (waves, structures, …)
- Coherent structures are present in tokamaks.
  - Blobs/voids: plasma filaments with large +/– $\tilde{n}$ and long lifetime.
- Existing studies on coherent structures are incomplete.
  - No interaction of structures with waves and zonal flow.
  - Millions of papers on blobs, very little attention on voids.
- Blobs/voids are created in pairs from edge gradient relaxation events (GREs).
- Void stay in the bulk plasma ⟶ a messenger from edge to core.

N. Bisai, 2023, RMPP

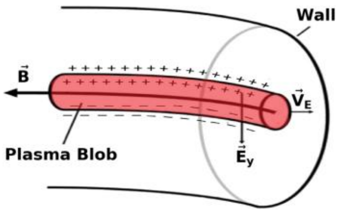

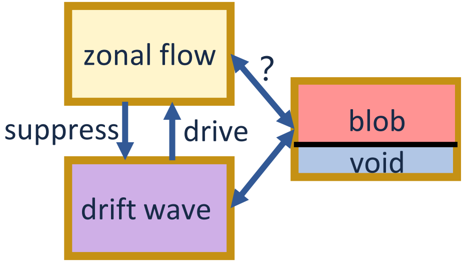

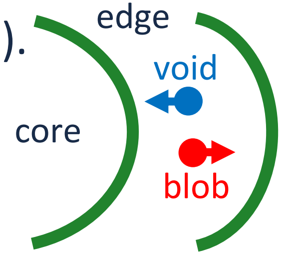

Motivation: edge-core coupling

- Physics of edge-core coupling: a critical problem for optimal plasma performance.
- Shortfall: turbulence level exceeds the prediction of Fickian gyrokinetic models.
    - Edge-core coupling region ⇒ a no man’s land.
- A “known unknown”: physics setting the width of the no man’s land.
- Tail wags the dog? A long history of speculation.

> “… And, finally, we have a very strong activity at the plasma edge. It controls the transition from one mode of confinement to another and its influence extends well into the bulk plasma… ” —B.B. Kadomtsev, 1992

- Can density void play a role in this process and address shortfall?

Motivation: edge-core coupling

- Experimental evidence from BES studies
- Bursts of zonal flow power usually follow the detection of density voids.

→ Density voids can drive zonal flow.

→ Need a model to figure out the role voids play in edge dynamics.

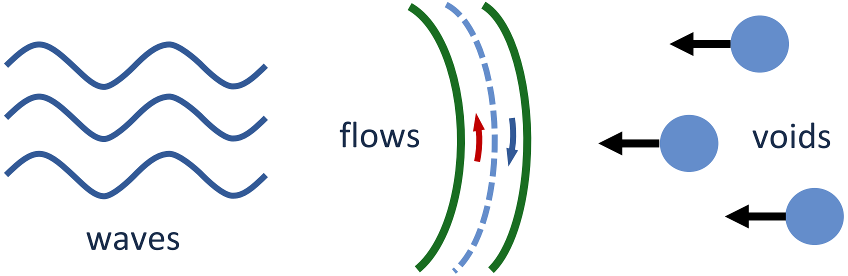

A. Sladkomedova, 2024, JPP

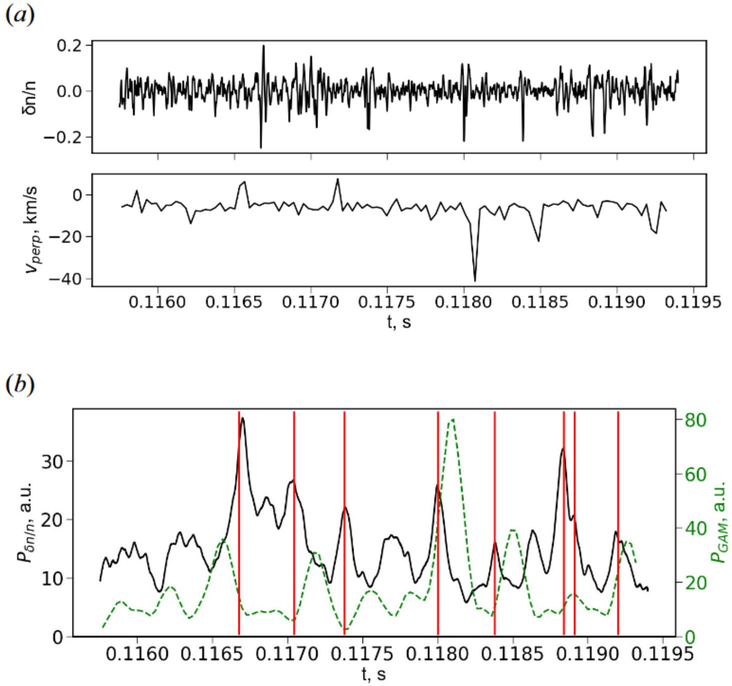

Scope

- Questions to address:
  1. What is the width of the turbulent layer (no man's land) driven by the voids?
  2. What are the mechanism and shearing rate of the void-driven zonal flow?
  3. How do (ambient) turbulence and zonal flow affect density voids?
- Three incentives:

Association

- An accelerating charge can emit EM wave → a moving void can be treated as a macro particle emitting waves.

Observation

- Radial propagation speed of voids is comparable to the diamagnetic drift velocity in the strong spreading scenario.[1]

Demand

- Connect to previous theoretical models of coherent structures, e.g., two-field model for structure convection.[2]

Picture: emission of drift waves from voids moving through the background plasma

⇒ start from Hasegawa-Wakatani model.

1. T. Long et al., 2024, NF.
2. O.E. Garcia et al., 2005, PoP.

Model: partition of the space

- Hasegawa-Wakatani model (with curvature drive):

$$\frac{d}{dt}\nabla_\perp^2\varphi + \frac{2\rho_s}{R_c}\frac{1}{n_0}\frac{\partial n}{\partial y} = D_\parallel\nabla_\parallel^2\left(\frac{n}{n_0} - \varphi\right)$$

$$\frac{1}{n_0}\frac{dn}{dt} = D_\parallel\nabla_\parallel^2\left(\frac{n}{n_0} - \varphi\right) \qquad \left(\alpha = \frac{D_\parallel\nabla_\parallel^2}{\partial_t}\text{: adiabaticity}\right)$$

- Divide the whole space into two parts:
  - Near field regime: $\alpha < 1$ (no adiabatic electrons)

$\Rightarrow$ Two-field model[1]: $\boxed{\frac{d}{dt}\nabla_\perp^2\varphi + \frac{2\rho_s}{R_c}\frac{1}{n_0}\frac{\partial n}{\partial y} = 0, \qquad \frac{1}{n_0}\frac{dn}{dt} = 0.}$

explains scaling of convection velocity

  - Far field regime: $\alpha > 1$

$\Rightarrow$ Hasegawa-Mima (HM) equation: $\frac{d}{dt}\nabla_\perp^2\varphi - \frac{1}{n_0}\frac{dn}{dt} = 0$

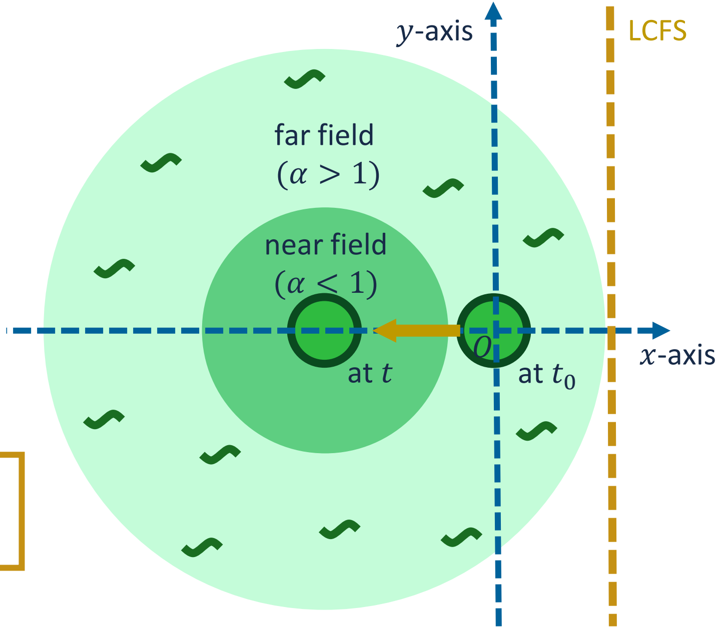

1. O.E. Garcia, 2005, PoP.

Model: local solutions of far field eqn

- Target: turbulence field excited by a moving void ⇒ focus on far field ($\alpha > 1$).
- Void enters via profile modulation, i.e., $n = n_0 + n_v + \tilde{n}$ (akin to test particle model)

$$\frac{d}{dt}(\nabla_\perp^2 \varphi - \varphi) - v_* \frac{\partial \varphi}{\partial y} = \boxed{\frac{1}{n_0}\frac{dn_v}{dt}} \rightarrow \text{source} \quad n_v = 2\pi n_0 h \Delta x \Delta y \delta(x + u_x t)\delta\left(y - u_y t\right) H(t) H(\tau_v - t)$$

h: magnitude; $\Delta x, \Delta y$: spatial extent; u_x, u_y: convection speed; τ_v: lifetime

- Workflow of the rest of the calculations:

Get the Green's func of the linearized H-M eqn and then solve φ of the far field equation → Estimate the void-induced turbulence intensity flux and width of the no man's land → Compare the shearing rate of the void-driven flow to the ambient shear (Reynolds stress)

Model: solutions of three cases

- Desired Green's function is obtained from geophysics (not plasma physics).
- Still meet two challenges:
  - Green's function is complicated. $G = -\int_{c-i\infty}^{c+i\infty} \frac{ds}{2\pi i} \exp\left(s\tau + \frac{v_* \chi}{2s}\right) \frac{1}{2\pi s} \mathrm{K}_0 \left[\left(1 + \left(\frac{v_*}{2s}\right)^2\right)^{1/2} \rho \right].$
  - Voids move in both x and y directions.
- Solution: consider three limiting cases:

a) Radially moving void $(u_y = 0)$:

  1) away from the x-axis ($|y| \gg |x|$)
  2) near x-axis ($|x| \gg |y|$)

b) Poloidally moving void $(u_x = 0)$:

  3) near y-axis ($|y| \gg |x|$)

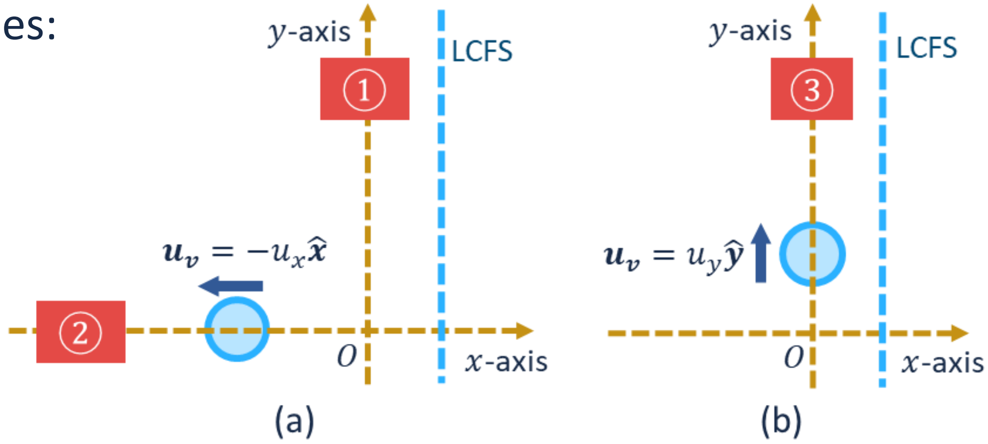

Results: width of no man's land

UC San Diego

- $|\psi_0 - \psi_1|$: penetration depth of voids.
- (ψ_2, ψ_1): edge-core coupling region (no man's land)
- Balance equation for turbulence intensity:
  - $\frac{\partial}{\partial t}\langle \tilde{v}^2 \rangle = -\frac{\partial}{\partial x}\langle \bar{\Gamma} \rangle + \kappa \langle \tilde{v}\tilde{n} \rangle$
- $\langle \bar{\Gamma} \rangle$: averaged turbulence intensity flux (over y and t).
- Integrating over NML:
  - $R_a = \frac{\text{nonlocal intensity flux}}{\text{local production}} = \frac{\langle \bar{\Gamma} \rangle|_{\psi_1}}{\int_{\psi_2}^{\psi_1} \kappa \langle \tilde{v}\tilde{n} \rangle dr} \approx \frac{\langle \bar{\Gamma} \rangle|_{\psi_1}}{\kappa \langle \tilde{v}\tilde{n} \rangle w_{nml}}$
- In NML, $Ra \sim 1 \Rightarrow$ NML width $w_{nml} \sim \langle \bar{\Gamma} \rangle|_{\psi_1} / \kappa \langle \tilde{v}\tilde{n} \rangle$.

l: spacing between emitters

Δy: width of emitters.

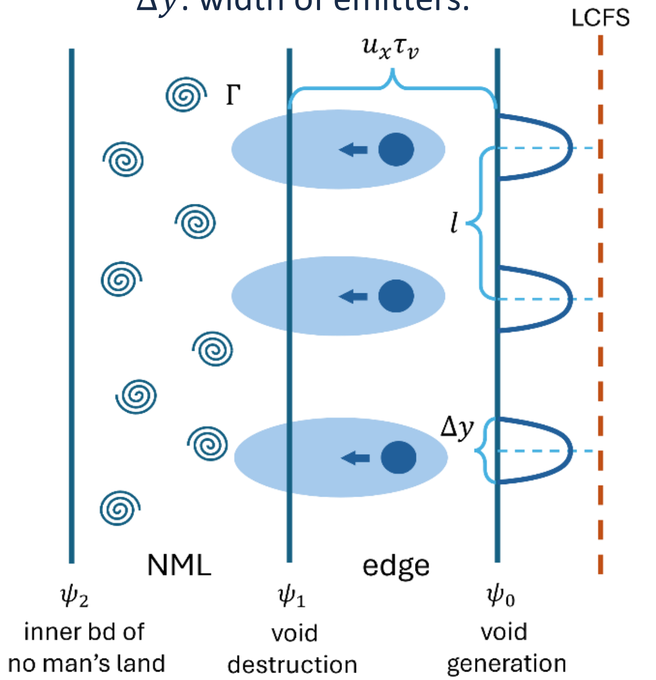

Results: width of no man's land

- GREs (edge instabilities) contain N troughs.
- After each waiting time τ_w, N voids are generated.
- Each void provides a turbulence intensity burst ΔI

$\rightarrow \Gamma = \sum_{i,j} u_x \Delta I 2\pi \Delta y \tau_v \delta(y - il)\delta(t - j\tau_w)$.

  - ΔI: evaluated from the local solution at $x \rightarrow \psi_1^-$ in case 2.

$$\rightarrow w_{nml} \sim \frac{2\pi}{\kappa\langle\tilde{v}\tilde{n}\rangle}\left(\frac{h\Delta x\Delta y}{u_x\tau_v}\right)^2 \frac{1}{v_*\tau_v^2}\frac{N\Delta y}{L_y}\frac{\tau_v}{\tau_w}.$$

- For $N \sim \mathcal{O}(1)$ (strong ballooning), $\Delta x \sim \Delta y \sim 10$, $u_x \sim v_* \sim 10^{-2}$, $\tau_v \sim 10^3$, $l \sim 10^3$, $\tilde{v} \sim \tilde{n} \sim 10^{-2}$, $\kappa/2\pi \sim 10^{-4}$, $h \sim .1 \rightarrow$ $\boldsymbol{w_{nml} \sim 10^2\rho_s}$.

l: spacing between emitters

Δy: width of emitters.

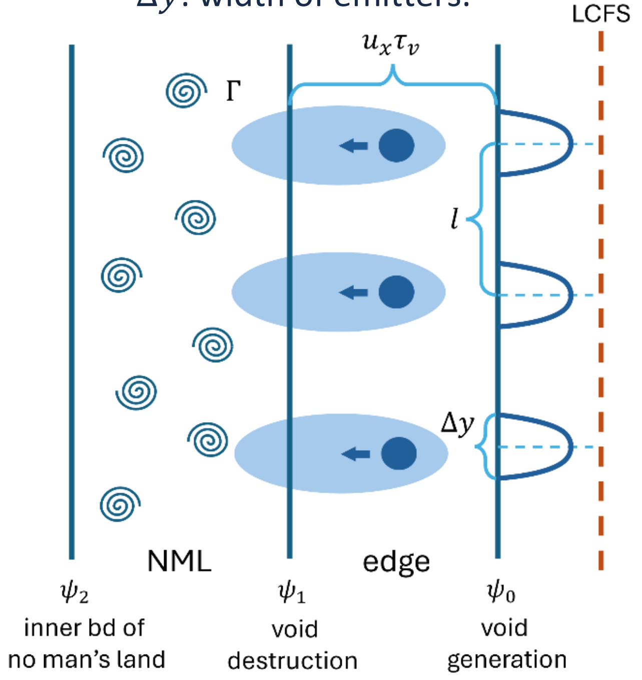

Results: shearing rate of void-driven flow

UC San Diego

- Summary of the shearing rates of zonal flow driven by voids ω_s^v in all three cases:

Case	ω_s^v/ω_s^a	If $v_F^a \sim v_*$, $\Delta_F^a \sim 10\rho_s$
$\boldsymbol{v_h} = -u_x\hat{\boldsymbol{x}}$ away from x-axis	$\frac{\omega_s^h}{\omega_s^a} \sim \left(\frac{h\Delta x\Delta y}{v_* u_x \tau_v a}\right)^2 \frac{\Delta_F^a}{v_F^a/v_*}$	$\frac{\omega_s^v}{\omega_s^a} \sim 10h^2$
$\boldsymbol{v_h} = -u_x\hat{\boldsymbol{x}}$ near x-axis	$\frac{\omega_s^h}{\omega_s^a} \sim \left(\frac{h\Delta x\Delta y}{v_* u_x \tau_v}\right)^2 \frac{2\ln(a/v_*)\,\Delta_F^a}{x^3 v_F^a/v_*}$	$\frac{\omega_s^v}{\omega_s^a} \sim (10h)^2 \quad \left(\frac{x}{\rho_s} \sim 10^2\right)$
$\boldsymbol{v_h} = u_y\hat{\boldsymbol{y}}$ near y-axis	$\frac{\omega_s^h}{\omega_s^a} \sim \frac{\pi}{2}\left(\frac{h\Delta x\Delta y}{v_* u_y \tau_v}\right)^2 \frac{x}{a^3} \frac{\Delta_F^a}{v_F^a/v_*}$	$\frac{\omega_s^v}{\omega_s^a} \sim h^2 \quad \left(\frac{x}{\rho_s} \sim 10\right)$

v_F^a: ambient flow velocity;
Δ_F^a: ambient flow width;
a: minor radius;
ω_s^a: ambient shearing rate

- As $h = n_v/n_0 \in (0.1,1)$, ω_s^v could be comparable to ω_s^a (exceed it in case 2).
- Order-of-magnitude estimate… but flexibility in choice of parameters indicates generality.

$$v_*/c_s \sim u_x/c_s \sim 2u_y/c_s \sim 10^{-2},\ a/\rho_s \sim 10^3,\ \omega_{ci}\tau_v \sim 10^3,\ t \sim 10^5$$

Results: void lifetime

- Effects of turbulence and flow on voids?
  - Turbulence/flow can smear/shear the void.
- Consider a passive diffusion: $\partial_t n_v = D\nabla_\perp^2 n_v$.
- A practical definition of the void lifetime:

→ half-life ⇒ $\tau_v = 2\Delta x^2/D$. $D \sim \tilde{v} l_{mix}$

- For $\rho_* = \frac{\rho_s}{L_n} \sim 0.01, \frac{\omega_s^a}{\omega_*} \sim \rho_*^{\frac{1}{2}}, \frac{\omega_*}{\omega_{ci}} \sim \rho_*$:
  - In purely diffusive regime ($\omega_s^a < Dk_\perp^2$ or $\frac{1}{2} < \delta < 1$): $\tau_v \propto \rho_*^{-\delta}$.
  - In shearing dominant regime ($\omega_s^a > Dk_\perp^2$ or $0 < \delta < \frac{1}{2}$): $\tau_v \propto \rho_*^{-(1+2\delta)/4}$.

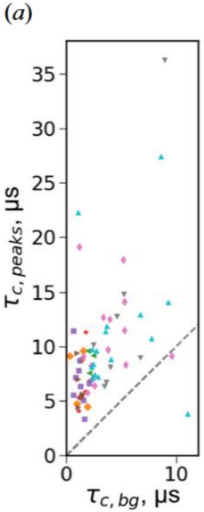

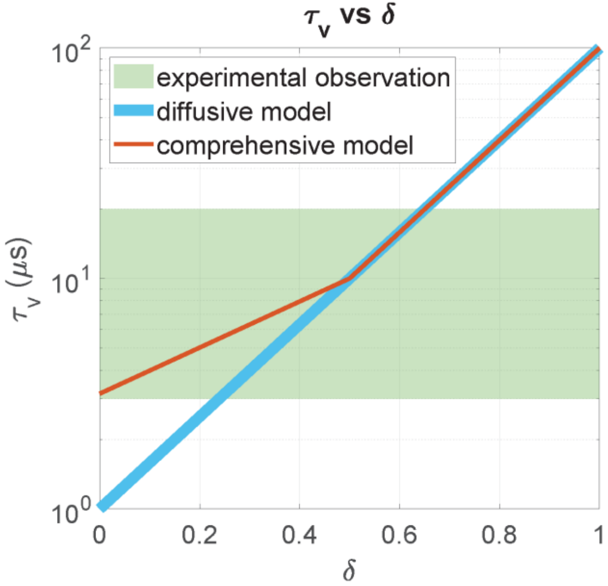

$\delta = \ln(l_{mix}/L_n)\,/\ln\rho_*$

- Our estimate: $\tau_v \sim 3 - 100\ \mu s$ vs. experiment: $\tau_v \sim 3 - 20\ \mu s$.

Section summary

- A theory incorporating density voids into turbulence dynamics.
  - It goes well beyond the traditional predator-prey model.
- How the tail (edge) wags the dog (core): emission of drift waves from moving voids drives substantial inward turbulence spreading and so drives a broad turbulent layer.
- More specifically, we calculate:
  - The width of the NML, which depends on the void parameters, is of order $100\ \rho_s$.
  - The shearing rate of the void-driven zonal flow is comparable to or even exceeds the ambient shear.
  - The void lifetime ranges from a few to $100\ \mu s$, which encompasses experimental values reasonably well.
- Expect results apply not only to L-mode, but also to H-mode ⇒ ELMs are also GREs![1]

1. Nami Li, et al., 2023, NF.

Summary and future research

Summary

$$\overbrace{\text{stochasticity, toroidicity}}^{\text{compound}}$$

Three new ingredients—stochasticity, toroidicity, and nonlocality—are added.

I. Theories of resistive interchange mode and quasi-mode in a stochastic magnetic field.

i. Microturbulence is driven to maintain quasi-neutrality at all scales.

ii. $\langle \tilde{b}_x \tilde{v}_x \rangle$ and $\langle \tilde{b}_y \tilde{v}_x \rangle$ develops $\Rightarrow$ noisier turbulence $\Rightarrow$ reduced complexity in experiments.

iii. Net effect of stochastic magnetic fields is to oppose mode growth $\Leftarrow$ enhanced by toroidicity.

II. Physics of edge-core coupling by void-induced inward turbulence spreading.

i. Emission of drift waves from moving voids drives substantial inward turbulence spreading.

ii. Nonlocal turbulence spreading could be comparable to local production $\Rightarrow w_{nml} \sim 100\ \rho_s$.

iii. Emitted drift waves can further drive zonal flow, with $\omega_s^v \geq \omega_s^a$.

iv. Voids are smeared and sheared by ambient turbulence and shear $\Rightarrow \tau_v$: a few to $100\ \mu s$.

Future research

Theoretical:

I. Kinetic description.

II. Incorporating zonal flow.

III. A fully self-consistent model (radiation reaction).

Experimental:

I. Complexity-entropy analysis for BES data.

II. Direct examination of $\langle \tilde{\boldsymbol{b}} \tilde{v}_x \rangle$.

III. Evidence of void–turbulence–zonal flow interactions (wavelet bispectrum analysis).

Only half of the story...... $\mathrm{Ku} = \frac{\tilde{V}\tau_{ac}}{\Delta}$

I. Ku $<$ 1 is adopted more or less.

II. Ku $\sim$ 1 for edge turbulence?

III. Realme of Ku $>$ 1 $\Rightarrow$ percolation?

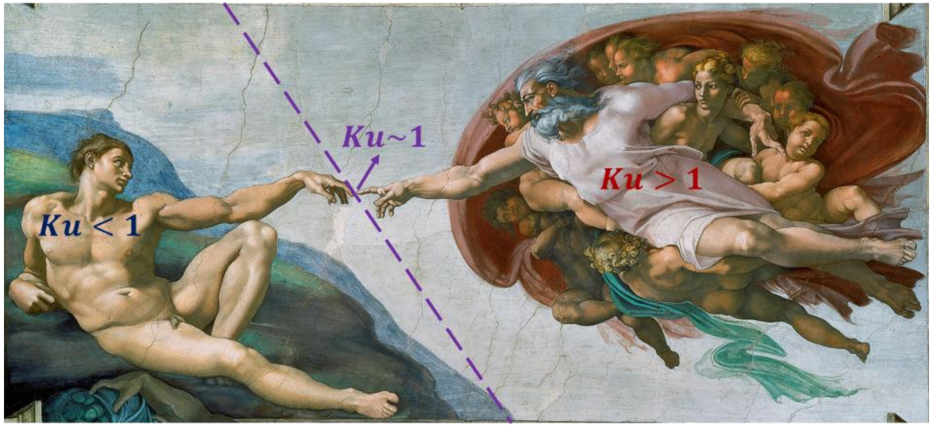

Acknowledgements

UC San Diego

- I sincerely thank my advisor, Prof. Pat Diamond, for his teaching, guidance and support during my Ph.D. education.
- I also thank the other professors of my committee for their help in my dissertation.

- Publications

1. Mingyun Cao and P.H. Diamond. “Instability and turbulent relaxation in a stochastic magnetic field.” *Plasma Physics and Controlled Fusion* 64, no. 3 (2022): 035016.
2. Mingyun Cao and P.H. Diamond. “Quasi-mode evolution in a stochastic magnetic field.” *Nuclear Fusion* 64, no. 3 (2024): 036003.
3. Mingyun Cao and P.H. Diamond. “Physics of Edge-Core Coupling by Inward Turbulence Propagation.” *Physical Review Letters* 134 (2025): 235101.

Thank you!